

# THE ASCAT ULTRA-HIGH RESOLUTION WIND PRODUCT

Jur Vogelzang, Ad Stoffelen, and Anton Verhoef

Royal Netherlands Meteorological Institute KNMI, Wilhelminalaan 10, 3732 GK De Bilt, Netherlands

## Abstract

An experimental ASCAT wind product on a 6.25 km grid size is presented and discussed. Operational production is not yet possible due to timeliness constraints, but these are expected to be solved with EUMETSAT's new ASCAT Full Resolution Product. The ASCAT-6.25 product is obtained by extending the processing used for the operational ASCAT coastal product. Some examples of the ASCAT-6.25 product clearly show its potential for detecting mesoscale features. The noise properties of the ultra-high resolution ASCAT-6.25 product are estimated. It is shown that the maximum noise variance is  $0.2 \text{ m}^2\text{s}^{-2}$  in the zonal wind component and  $0.3 \text{ m}^2\text{s}^{-2}$  in the meridional wind component. The new ASCAT Full Resolution Product is expected to be issued in 2013, and an experimental version of the ASCAT-6.25 product will become routinely available for the user community in 2013/2014.

## INTRODUCTION

Numerical Weather Prediction (NWP) models and nowcasting applications require increasing resolution in meteorological information, both in space and time. Particularly, in extreme weather conditions the signal gradients are large and intense small-scale wind features may stand out above the noise floor. The ASCAT scatterometer on board Metop-A produces radar measurements that - when recorded above sea - are converted into accurate ocean surface wind speed and directions. Originally, the wind information was disseminated by the Ocean and Sea Ice satellite Application Facility (OSI SAF) only on a 25 km by 25 km grid (ASCAT-25). Soon after that, a product on a 12.5 km grid was introduced (ASCAT-12.5), followed by the ASCAT coastal product a few years ago. The ASCAT coastal product also has a grid size of 12.5 km, but since the averaging procedure for obtaining radar cross sections was redesigned, using EUMETSAT's full resolution product and an accurate land/sea mask, the wind information extends further to the coast than for the ASCAT-12.5 product.

The gridded radar cross section products for ASCAT-25 and ASCAT-12.5 are generated by EUMETSAT. All ASCAT wind products are generated by the ASCAT Wind Data Processor (AWDP), a software package developed within the Satellite Application Facility for Numerical Weather Prediction (NWP SAF). AWDP can be obtained free of charge upon registration. The coastal processing in AWDP can easily be adapted to generate a product on a 6.25 km grid. The grid size may even be diminished further, though the size of the antenna footprint imposes a firm limit.

In section 2 we describe the ASCAT processing, in particular the steps from the full resolution radar measurements to a gridded radar cross section product that is input for the wind processing. The differences between ASCAT-25, ASCAT-12.5, and ASCAT-coastal are presented, and it is shown how an ASCAT-6.25 km product may be constructed. Quality control for the ASCAT-6.25 km product requires readjustment of some incidence angle dependent parameters in AWDP. Since the current processing is too slow to meet the operational requirements, it was decided to simulate the noise properties of ASCAT-6.25 using the coastal product. These results are presented in section 3. Section 4 gives a few examples of ASCAT-6.25 scenes that demonstrate its capabilities for detecting mesoscale features. The paper ends with the conclusions.

## PROCESSING

Being a fan beam scatterometer, a single pulse of ASCAT illuminates an elongated oval region that is chopped electronically in the range direction using the time of arrival of the return signal. The basic radar measurements, further referred to as single look measurements, cover an area of about 5 km × 20 km. The single look measurements are gridded to a level 1 radar cross section product. The procedure is as follows (see also figure 1):

1. An averaging area (green shaded oval in figure 1) is defined for each grid cell (grey square in figure 1)
2. The centre of each single look measurement is determined. The single look measurements are represented in figure 1 by solid black ellipses for the forward beam and the dashed black ellipses for the aft beam (assuming the range direction from top to bottom; the mid beam is omitted).
3. If the centre of a single look measurement falls within the averaging area of a certain cell, it is attributed to that cell (“drop-in-the-bucket method”).
4. The radar cross sections of all single look fore beam measurements attributed to a grid cell are averaged to yield the gridded radar cross section and similarly so for mid and aft beam.

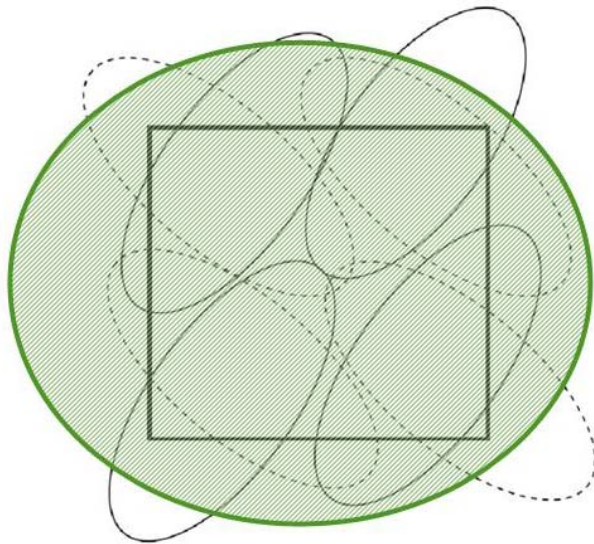


**Figure 1: Scheme of the calculation of gridded radar cross sections. The averaging area is shaded green. The black square represents the grid cell, while the ellipses represent the single look measurements. See text for details.**

It should be noted here that the averaging area is in general larger than the grid cell to allow for some oversampling, a procedure common in most radar applications. Therefore a single look measurement may attribute to more than one grid cell. Further, the averaging area may have any shape, though physical and practical considerations limit the shape to squares and circles.

The left hand side panel of figure 2 illustrates the cross section gridding procedure for ASCAT-25 and ASCAT-12.5. The averaging area is a square centred at the grid cell of size 100 km × 100 km for ASCAT-25 and size 50 km × 50 km for ASCAT-12.5. The gridded radar cross sections are obtained by averaging the single look measurements with a Hamming weight function in both directions, so that single look measurements in the central part of the averaging area have highest impact.

The right hand side panel of figure 2 illustrates the gridding procedure for the ASCAT coastal product. Here the averaging area is a circle with radius  $R = 15$  km centred at the middle of the grid cell. Single look measurements attributed to a cell are simply averaged. By using a high resolution land/sea mask, denoted by the orange line in figure 2, single look measurements over land are excluded. Since the land/sea discrimination is now at the level of single look measurements, rather than on the level of gridded radar cross sections, wind information closer to the coast can be obtained. The value of  $R$  was chosen such that the coastal product has (almost) the same characteristics as the ASCAT-12.5 product in regions far away from the coast.

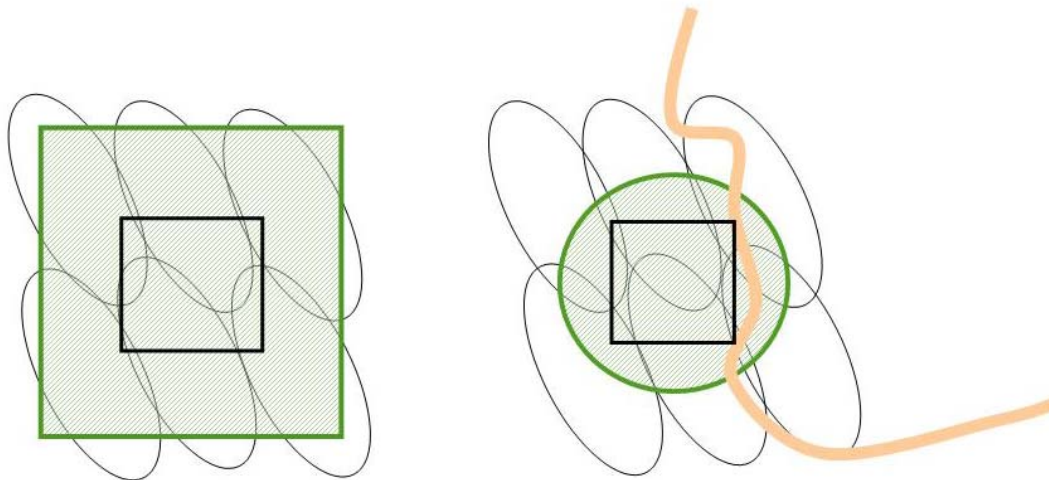


**Figure 2:** Radar cross section gridding for the ASCAT-25 and ASCAT-12.5 products (left) and for the coastal product (right).

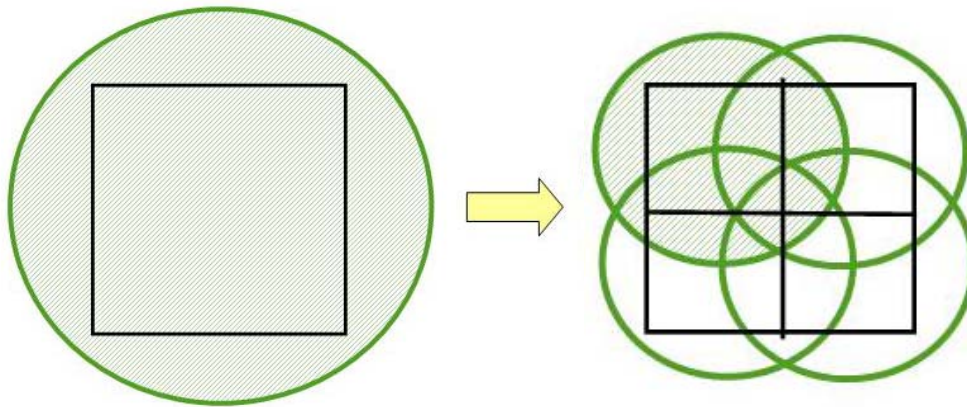


**Figure 3:** From the coastal product (left) to the ASCAT-6.25 (right). The single look measurements and some of the averaging area shading have been omitted.

An obvious extension to the radar cross section gridding in the coastal product is to split one grid cell into four and to take  $R = 7.5$  km, as depicted in figure 3. This leads to the ASCAT-6.25 km product. However, computation time becomes a limiting factor. The current full resolution product is organised such that it must be searched (or at least a part of it) for each grid cell separately. Increasing the number of grid cells by a factor 4 also increases the time needed for searching single look measurements attributed to a grid cell. This increase in computation time prohibits operational implementation at this stage. This problem will be handled after EUMETSAT has started production of a new full resolution product.

Figure 4 shows the first ASCAT-6.25 result (right hand panel) together with the coastal product (left hand panel). Both panels cover the same area of  $4^\circ$  by  $4^\circ$  northeast of the Philippines, recorded by ASCAT on January 26, 2012 around 00:36 UT. Blue arrows denote wind vectors that passed all quality controls. Orange arrows were flagged by the KNMI MLE check, indicating that the radar cross sections are too far apart from the values expected from the wind estimates. This is mostly caused by sea ice or, in this case of a tropical cyclone, by extreme rain or confused sea state. Purple arrows indicate wind vectors that were flagged by the variational quality control, indicating a large deviation of the local scatterometer wind from the 2DVAR analysis.

The ASCAT-6.25 product shows some convergence lines that look realistic and are not easily visible in the coastal product. It also shows that quality control needs to be retuned. This is no surprise, as the quality control in AWDP contains incidence angle dependent parameters.

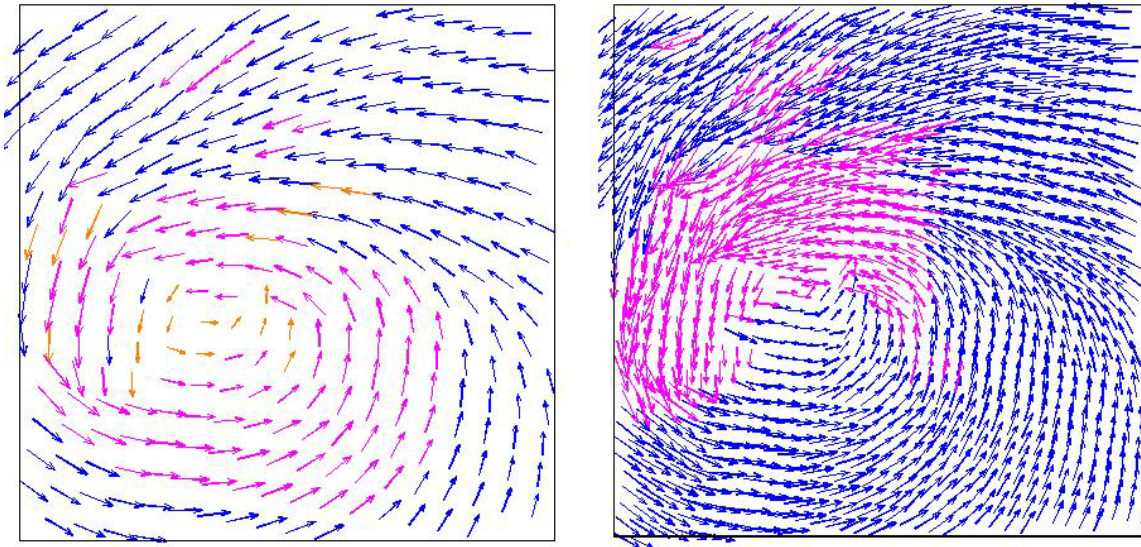


**Figure 4:** Tropical cyclone observed on January 26, 2010 around 00:36 UT by ASCAT. Left: ASCAT coastal product; right: first ASCAT-6.25 result. Blue arrows denote wind vectors that passed all quality checks. Orange arrows were flagged by the MLE quality control, while purple arrows were flagged by the variational quality control.

## NOISE CHARACTERISTICS

It is very well possible to tune quality control for an ASCAT-6.25 product, but since computation time prohibits operational use at this stage, it was decided not to put effort in this until the advent of the new full resolution product. Nevertheless, it is possible to study some of the quality aspects of the ASCAT-6.25 product with well-tuned quality control, by considering the coastal product (12.5 km grid size) with different values for  $R$ . Figure 5 shows the noise variances

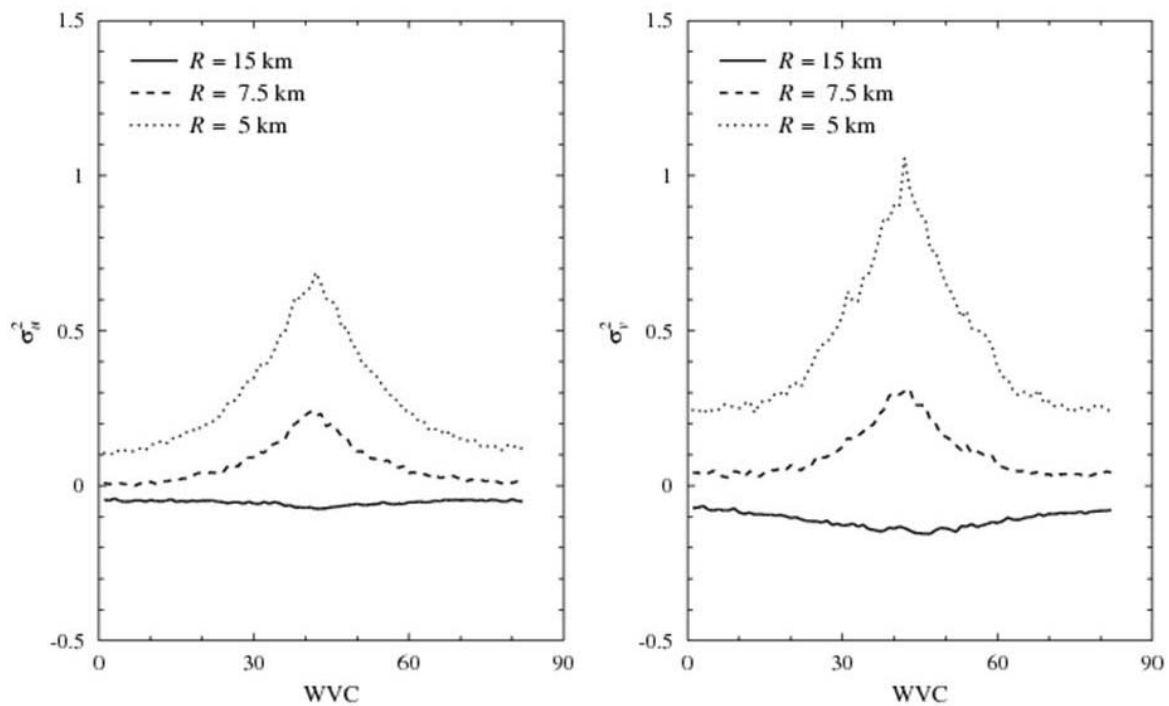


**Figure 5:** Noise variance in the zonal wind components  $u$  (left) and  $v$  (right) of the coastal product as a function of Wind Vector Cell number (WVC) for various values of  $R$ .

The noise variances in figure 5 were obtained from all ASCAT data in the period April 2-8, 2010. The autocorrelation was calculated for each wind component and extrapolated to zero distance (Vogelzang et al., 2009). For  $R = 15$  km, the value used for the coastal product, the noise variances are slightly negative. This indicates that the ambiguity removal step not only filters out noise, but also removes some small scale signal. For  $R = 7.5$  km the noise variances becomes positive. The highest values,  $0.2 \text{ m}^2\text{s}^{-2}$  for  $u$  and  $0.3 \text{ m}^2\text{s}^{-2}$  for  $v$ , are obtained for the smallest incidence angles (Wind Vector Cell numbers 41 and 42). Further reducing  $R$  to 5 km increases the noise variance considerably. This is as expected, because reduction of  $R$  reduces the number of single look measurements contributing to the gridded radar cross section.

One may therefore expect that the ASCAT-6.25 km product contains more noise than the ASCAT-12.5 or coastal products. If the noise level affects product quality too much it is possible to apply the so-called Multi Solution Scheme (MSS) that has been applied to QuikSCAT earlier (Portabella and Stoffelen, 2004; Vogelzang et al., 2009).

## SOME EXAMPLES

Figure 6 shows an experimental ASCAT-6.25 scene recorded on April 2, 2010 in the Indian Ocean north of the Kerguelen Islands. Quality control flags have been ignored. The scene shows a wavy front line that is sharp in the western part but becomes smoother to the east. The wind field north of the front looks quite homogeneous, but south of the front there are several wavy patterns and convergence/divergence zones.

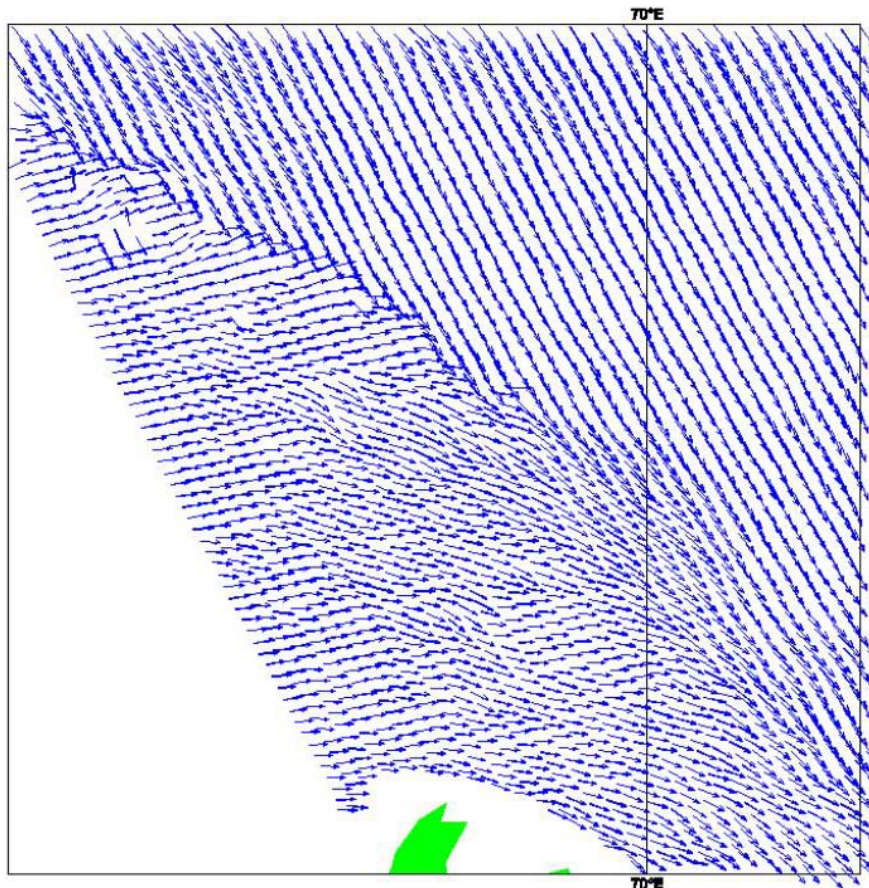


**Figure 6:** ASCAT-6.25 scene recorded April 2, 2010 in the Indian Ocean north of the Kerguelen Islands. The scene measures  $5^\circ$  by  $5^\circ$  and is centred around  $-47^\circ$  latitude and  $69^\circ$  longitude.

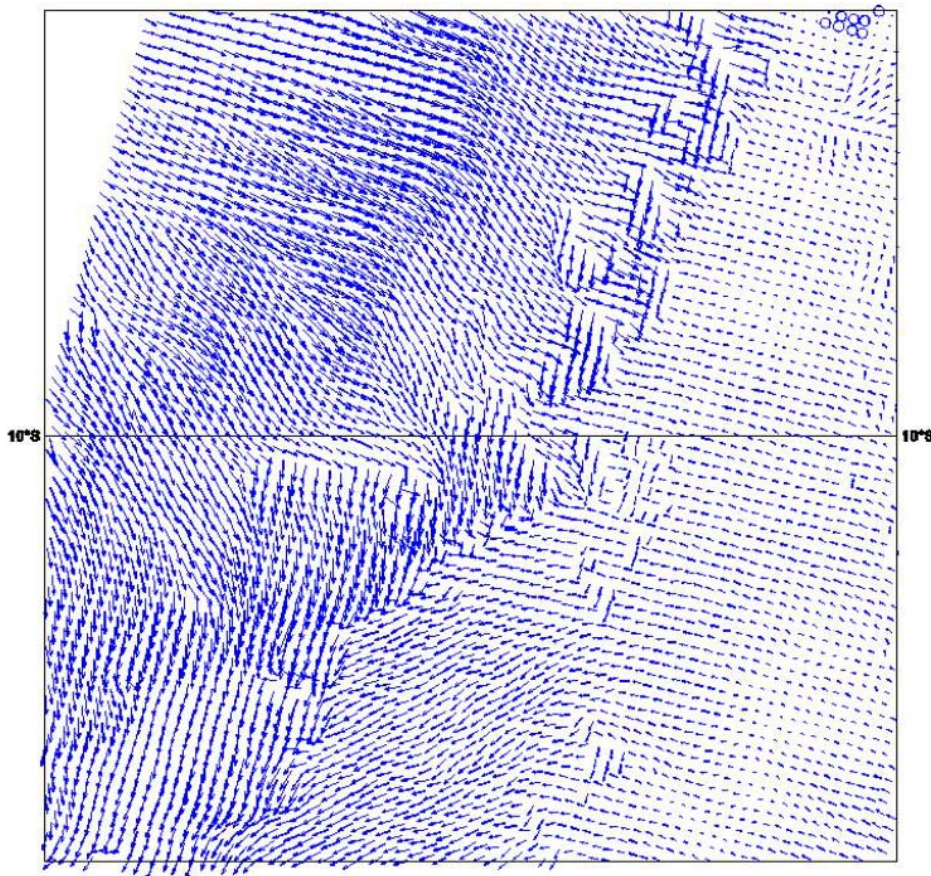


**Figure 7:** ASCAT-6.25 scene recorded April 2, 2010 in the Indian Ocean. The area measures 4° by 4° and is centred at -10° latitude and 102° longitude.

Figure 7, recorded April 2, 2010, also shows a frontal area in the Indian Ocean with an even richer structure. The signatures along the front may be caused by showers or downdrafts, but may also indicate poor data quality. It is clear that more research is needed in order to fully characterise the quality of the ASCAT-6.25 product. Nevertheless, figures 4, 6, and 7 indicate the potential of such a product for observing mesoscale features.

It is in principle possible to generate wind products on smaller grid sizes than 6.25 km. However, this makes little sense in practice: such a product does not reveal additional details because the grid size becomes smaller than the size of the single look measurements. Moreover, as the averaging area decreases, the noise level increases. A 6.25 km grid seems the smallest possible choice.

## CONCLUSIONS AND OUTLOOK

An experimental ASCAT wind product with a grid size of 6.25 km has been presented. The product looks very promising for observation of mesoscale features. It is created by extending the processing currently used for the ASCAT coastal product. The ASCAT-6.25 product contains more noise than the coastal product, about  $0.2 \text{ m}^2\text{s}^{-2}$  in  $u$  and  $0.3 \text{ m}^2\text{s}^{-2}$  in  $v$  for the smallest incidence angles, but this is not prohibitive.

The ASCAT-6.25 km product needs EUMETSAT's full resolution product for regridding the radar cross sections, just like the coastal product. At this stage computation time is a prohibiting factor for operationalising the ASCAT-6.25 product. This is a technical problem that will be handled after. EUMETSAT has started dissemination of the new full resolution product in 2013. Experimental dissemination of the ASCAT-6.25 product will follow after about six months, in 2013/2014.

## **ACKNOWLEDGEMENTS**

This work was supported by EUMETSAT within the Satellite Application Facility for Numerical Weather Forecast (NWPSAF).

## **REFERENCES**

Portabella, M. and A. Stoffelen, (2003) A probabilistic approach for SeaWinds data assimilation. Q.J.R. Meteorol. Soc., **130**, pp. 1-26. doi: 10.1256/qj.02.205

Vogelzang, J., A. Stoffelen, A. Verhoef, J. de Vries, and H. Bonekamp, (2009) Validation of two-dimensional variational ambiguity removal on SeaWinds scatterometer data. J. Atm. Ocean. Tech., **26**, pp. 1229-1245. doi: 10.1175/2008JTECHA1232.1.